16th World Conference on Earthquake, 16WCEE 2017
Santiago Chile, January 9th to 13th 2017
Paper N° 4888
Registration Code: S-D1463165524

QUANTITATIVE EVALUATION OF NEW STRATEGIES TO INCREASE SEISMIC RESILIENCE OF CITIES: A SHIFT OF CURRENT PARADIGMS

P. Heresi[(1)], E. Miranda[(2)]

[(1)] PhD Candidate, Dept. of Civil and Environmental Engineering, Stanford University, Stanford, CA, USA, pheresi@stanford.edu
[(2)] Associate Professor, Dept. of Civil and Environmental Engineering, Stanford University, Stanford, CA, USA, emiranda@stanford.edu

Abstract

Lowrise wood-frame structures represent the most frequently used construction type for residences in many earthquake-prone regions such as the United States, Japan, Canada, New Zealand and many other countries. Although in general these structures have shown an acceptable seismic performance in terms of collapse safety, they have resulted in multi-million dollar losses that have large regional economic impact. Furthermore, even if collapse is avoided, damage may result in occupants being displaced from their residences, which for urban areas translates into the need to provide temporary housing to many thousands of people. Investigators at Stanford University have recently developed a new approach, referred to as "unibody design" which allows to significantly increase the lateral strength but particularly the lateral stiffness of lightweight residential construction, with very small increases in cost and changes in construction practice. Contrary to current approaches that allow significant nonlinear behavior and damage to take place, the unibody approach allows lowrise wood structures to essentially remain elastic and nearly damage free even in the event of large earthquakes. This paper proposes a probabilistic performance-based earthquake engineering framework for quantifying the benefits at a regional scale of using an enhanced design, in this case the unibody design, in residential construction. This study demonstrates that benefits of this novel approach are nonlinear, generating an exponential chain of regional risk reduction. Reasons for these large benefits are explained, as four effects can be superimposed: (1) increase the stiffness and strength significantly reduces the displacement demands in short-period structures, (2) reduced displacement demands result in a lower probability of damage, (3) enhanced houses closer to the seismic source present similar damage probabilities as conventional houses much farther away, and (4) the difference in distances to the seismic source are translated into significant differences in affected areas, and therefore, the number of damaged houses. The proposed framework is not exclusive of the unibody approach and can be used for evaluating the benefits of different types of retrofits or new designs which increase the strength and the stiffness of houses in an urban area. This framework provides useful information for decision-makers in seismic-prone regions to evaluate new public policies and the resilience of the residential construction.

Keywords: regional risk estimation; residential construction; performance based earthquake engineering; resilience

1. Introduction

Wood-frame dwellings represent the most frequently used construction type for residences in many earthquake-prone regions. According to the World Housing Encyclopedia (WHE) [1], wood-frame houses constitute around 98% of existing and new houses in Western USA, 56% of the building stock in the Province of British Columbia, Canada, and in 1998 they were more than the 53% of the houses in Japan. Moreover, wooden houses also constitute the majority of the residential building stock in New Zealand [2]. Even though engineered low-rise residential constructions have an acceptable performance in terms of collapse safety, large economic losses due to damage repair may be unacceptable and virtually bankrupt house owners. For example, the M6.7 1994 Northridge earthquake produced widespread damage in the Los Angeles metropolitan area, especially in light wood-frame houses. More than 40,000 housing units were yellow-tagged and 16,000 units were red-tagged in Los Angeles County alone [3], and the total residential losses were between approximately $13 and $20 billion dollars [4 – 7]. The M6.6 1971 San Fernando earthquake, which damaged more than 20,500 houses, produced losses to single-family houses of approximately $114.4 million dollars, excluding land and contents [8, 9]. In both earthquakes (1994 Northridge and 1971 San Fernando) losses to single-family houses were larger than losses in any other building category. Moreover, according to Jennings [10] the real losses in residential construction were probably much greater than those reported in damage surveys after earthquakes. Another example is the M6.9 Kobe earthquake, in 1995, which damaged more than 400,000 housing units and produced between $45 and $75 billion dollars of residential losses [4]. Additionally, Kircher et al. [11] estimate that about 160,000 – 250,000 households could be displaced from damaged residences in a repeated event of the 1906 San Francisco earthquake, magnitude 7.9. These examples show how inadequate seismic performance can have an enormous impact to society in the aftermath of an earthquake happening near large urban areas. Houses heavily damaged and yellow- or red-tagged, limiting their occupancy, significantly affect the seismic resilience. Thus, a key factor for increasing the resilience of cities after earthquakes is the improvement of the performance of low-rise residential construction on a regional scale.

Many researchers have investigated the benefits of different methods for retrofitting low-rise residential construction. For instance, Porter et al. [12] as part of the CUREE - Caltech Woodframe Project, analyzed the cost-effectiveness of different kinds of improvements (retrofit, redesign and improve quality) in wood-frame buildings. Other studies have demonstrated the influence of wall finish materials in the strength and the stiffness of shear walls [13 – 15]. Moreover, during the last five years, researchers at Stanford University have been working on a new design methodology for houses, referred to as the “unibody approach” (in relation to the transition from body-on-frame to unibody construction which occurred in the automobile industry during the 1970s). Gypsum partition panels and stucco cladding are strongly attached and explicitly designed to be part of the lateral resisting system of the structure [16 – 18]. Swensen et al. [17] propose a novel, yet simple method for achieving this, using inexpensive adhesive and enhanced screws between the sheathing and the frame of walls. The unibody design has been tested in full-scale rooms [19] and a full-scale 2-story house [20] with promising results.

This study proposes a performance-based earthquake engineering (PBEE) framework for quantifying the benefits at a regional scale of using an enhanced design (for example, the unibody design) in residential construction. The PBEE framework explicitly considers different sources of uncertainties and, as noted by May [21], it includes the societal benefit of providing performance information for future seismic design and risk management. In this sense, the objective of this framework is to provide more information for hypothetical new public policies to improve resilience in seismic regions. Results show that stiffer and stronger walls reduce the inelastic displacement demands for a given earthquake. This effect is maximized in short-period structures like lowrise single-family houses. The reduced displacement demand is then translated into a much lower probability of damage in each structure. With larger lateral stiffness and strength, enhanced houses closer to the seismic source will now present the same probability of damage as conventional houses that are much farther away. Thus, the affected area and the number of residential units with a given level of damage is greatly reduced. This study demonstrates that nonlinear relationships can be superimposed to generate an exponential chain of regional risk reduction.

2. Regional Loss Reduction Effects

This section describes the concepts that produce a large impact of using unibody construction at a regional scale. For this, houses with conventional construction method are compared with those with unibody approach, and different effects are considered. The unibody design is assumed to increase the stiffness 2 times and the strength by 50%. These hypothetical increments are consistent with empirical results for the unibody approach [16 – 20]. For all the following computations, the damping ratio is 10% (consistent with the damping measured by Camelo [22]), the story height is 2.4 meters, and the average shear wave velocity in the top 30 meters of soil, V_{S30}, is 250 m/s (NEHRP site class D). Furthermore, other values of damping ratio, story height and V_{S30} result in the same conclusions presented here.

2.1 Influence of Stiffness and Strength on Inelastic Displacement Demands

Inelastic displacement demands can be computed through nonlinear time-history analysis of a given structure subjected to an earthquake record. Nevertheless, in regional risk assessments this would require modeling each house separately, selecting adequate records for each one, and performing a large number of analyses. Therefore, inelastic displacement demands, Δ_i, can be estimated using simplified elastic single-degree-of-freedom (SDOF) systems, as shown in Eq. (1).

$$\Delta_i \approx C_R \cdot S_d \tag{1}$$

where S_d is the elastic spectral displacement and C_R is the inelastic displacement ratio for a given relative strength, R (Eq. (2)):

$$R = \frac{S_a}{C_y \cdot g} \tag{2}$$

where S_a is the pseudo-spectral acceleration ordinate, C_y is the normalized yield strength (that is the lateral yielding strength of the system, F_y, normalized by the weight of the structure, W) and g is the acceleration due to gravity. Moreover, the spectral displacement S_d can be written as a function of the pseudo-spectral acceleration ordinate and the period of the structure, T (which is itself a function of the mass and stiffness of the structure, M and K, respectively). These relationships are presented in Eq. (3).

$$S_d = \frac{S_a \cdot T^2}{4\pi^2} = S_a \cdot \frac{M}{K} \tag{3}$$

Note that S_a is also a function of the period T (and consequentially, also a function of the stiffness). If S_a is assumed to remain constant when doubling the stiffness, then the spectral displacement ordinate would be decreased 2 times. But S_a is not necessarily the same value after the stiffness is increased, and this depends on the spectral shape. Spectral shape (S_a normalized with respect to the peak ground acceleration, PGA) has been widely studied, and an example from Graizer and Kalkan [23] is presented in Fig. 1, for a set of magnitudes and distances. As can be seen, on average spectral shapes have a peak at periods between 0.2 and 0.7 seconds, with an ascending branch before the peak, and a descending branch after it. If the period of the structure is lower than the period of the peak and the stiffness is increased (thus reducing the period), the pseudo-spectral acceleration is reduced. As measured by Camelo [22], conventional 1-story houses have periods of around 0.1 seconds, and 2-story houses around 0.2 seconds. Therefore, and as a general trend, the fundamental periods of single-family houses lay in the ascending branch, where increasing the stiffness reduces the pseudo-spectral acceleration. For example, a reduction of the fundamental period from 0.10 seconds to 0.071 seconds (doubling the stiffness)

produces a reduction of S_a of, on average, approximately 1.2 times (note that this value varies for different combinations of magnitude and distance). This reduction is multiplied by the one due to the increase in stiffness in Eq. (3), mentioned above, producing a total reduction of more than 2.4 times (reduction of 58%) in the spectral displacement ordinate when merely doubling the stiffness. Note that even for periods slightly larger than the period of the peak in the spectral shape (thus at the start of the descending branch), if the stiffness is increased enough to move the period to the ascending branch, it could also result in a lower value of S_a. As can be observed, the reduction of the spectral displacement ordinate depends on the period of the structure. For long-period structures (at the descending branch of the spectrum), S_a increases when the stiffness is doubled, and the reduction of the spectral displacement is, for different combinations of magnitude and distance, merely between 20% and 40% (between 1.25 and 1.7 times). However, for short-period structures the spectral displacement is reduced, on average, by 40% to 60% (between 1.7 and 2.5 times), for different magnitudes and distances.

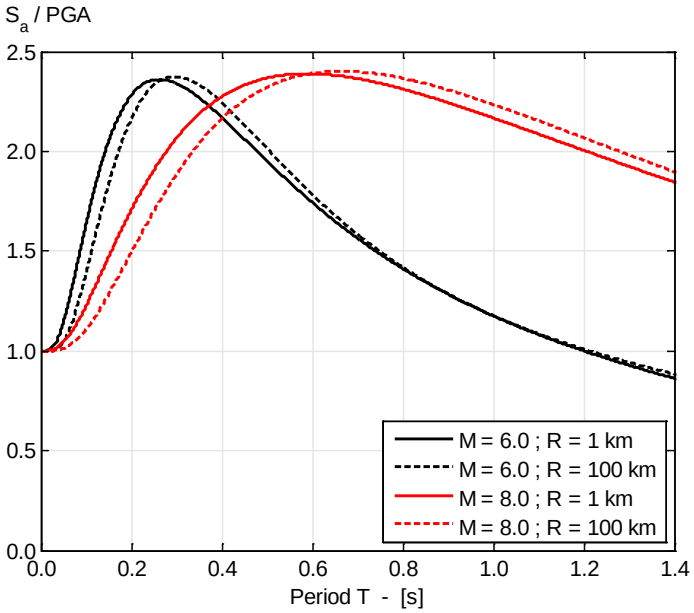

Fig. 1 – Spectral shapes for V_{S30} = 250 m/s and a set of magnitudes and distances, according to Graizer and Kalkan [23]. The peaks are presented at periods between 0.2 and 0.7 seconds.

On the other hand, Ruiz-García and Miranda [24, 25] performed a statistical analysis of C_R. The authors show that C_R is a random variable which is a function of the site class, the fundamental period of the structure (T) and its relative strength (R). Ruiz-García and Miranda not only suggest an expression for the central tendency of C_R, but also one for its dispersion. Furthermore, they noted that C_R is lognormally distributed. Akkar and Miranda [26] propose an improvement for C_R in the short period range. The authors suggest a correction term, C_f, as a function of the site class, the fundamental period of the structure (T), its relative strength (R), the spectral velocity (S_v) and the peak ground velocity (PGV) of the record. With this information, the inelastic displacement demand can be estimated with Eq. (4):

$$\Delta_i \approx \frac{C_R}{C_f} \cdot S_d \tag{4}$$

As can be seen in the previous equations, for a given set of record parameters (S_a, S_d, S_v and PGV) and a site class, the inelastic displacement demand is a function of the fundamental period of the structure (T) and its normalized strength (C_y). Finally, to estimate the record parameters, ground motion prediction equations

(GMPEs) can be used for a given magnitude and distance. Note that, in general, GMPEs do not provide estimates for S_v, but the pseudo-spectral velocity ordinate (PS_v) can be used as an approximation.

For a given set of record parameters, the effect of increasing C_y on the factor C_R/C_f of Eq. (4) depends on the period of the structure. For medium- and large-period structures, the effect of increasing the strength is, on average, negligible (this is known as the "equal-displacement rule", where inelastic displacements are on average similar to the elastic displacements in medium- and long-period structures). Nevertheless, increments in the lateral strength have a large impact in short-period structures: increasing the strength in 50% reduces the factor C_R/C_f by 30% to 60% (between 1.4 to 2.5 times).

To illustrate the effects of strength and stiffness increments in the inelastic displacement demands, Fig. 2 shows an example of median inelastic interstory drift ratio, IDR (that is the median inelastic displacement demand normalized by the story height), as a function of the fundamental period, for two different normalized yield strengths, and for a magnitude 7.0 earthquake and 2 km of source-to-site distance. The GMPE developed by Boore et al. [27] for the NGA-West2 project was used to obtain the record parameters (S_a, S_d, PS_v and PGV). Point 1 in Fig. 2 corresponds to the conventional construction, taken, as an example, as a system with a period of 0.10 seconds and a normalized strength of 0.4, where the median IDR is 0.183%. If the stiffness is doubled (Point 2), the median IDR is decreased to 0.091% (decreased by slightly more than 2.0 times or a reduction of 50%). If only the strength is increased by 50%, from 0.4 to 0.6 (Point 3), the median IDR decreases to 0.083%, (decreased by 2.2 times or a reduction of 55%). Finally, if both the strength and the stiffness are increased simultaneously (for example using a unibody design, Point 4), the median IDR is decreased to 0.030%, which corresponds to a reduction of 6.1 times (reduction of 84%). As a summary, in this example doubling the stiffness reduces the displacement demand by more than 2.0 times, while only increasing the strength by 1.5 times reduces the displacement by 2.2 times. Finally, a combination of both effects results in a reduction of the median displacement demand of 6.1 times. Note how this short-period structures takes full advantage of both increments, and the combination of both results in a reduction of more than 2.0 x 2.2 = 4.4 times.

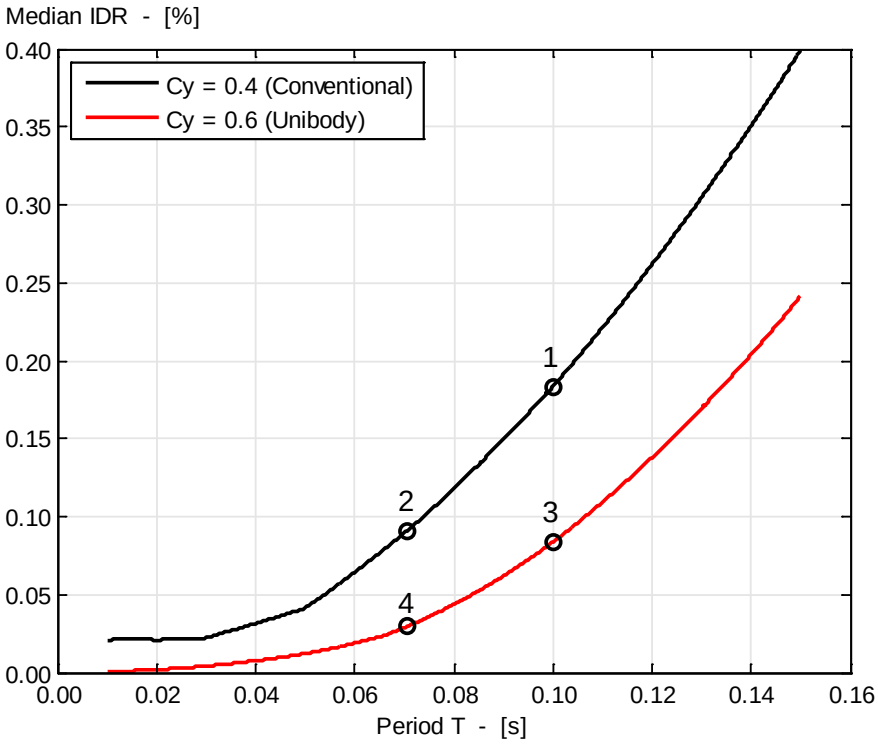

Fig. 2 – Median IDR as a function of fundamental period and normalized strength, for a magnitude 7.0 earthquake and source-to-site distance 2 km, using the GMPE by Boore et al. [27]. Point 1 corresponds to conventional construction, Point 2 to increased stiffness, Point 3 to increased strength and Point 4 to unibody approach (increased stiffness and strength simultaneously).

2.2 Influence of Inelastic Displacement Demands on Probability of Damage

Fragility curves are used to compute the probability that a certain component or group of components presents a given level of damage. These curves relate an engineering demand parameter, in our case IDR, with the probability of having a certain damage state *k*, DS_k, or higher. This relationship is usually described by lognormal cumulative distribution functions. An example of a fragility curve as a function of IDR is shown in Fig. 3. This curve was proposed by the ATC-58 project [28] for damage state 1 (DS_1) of light framed wood shear walls with structural panel sheathing (OSB or plywood), with exterior stucco finish and interior gypsum wallboard, designed with hold-downs (component number B2011.102 of ATC-58). The damage state DS_1 corresponds to cracking of stucco. Note that this component is used as an example of drift-sensitive damage in wood-frame houses, but any other or a combination of others might be used for estimating the total damage of houses. As in the previous section, a 7.0 magnitude earthquake and a site at 2 km from the rupture zone are taken to compare the conventional and unibody approaches. As can be observed, the probability of damage state DS_1 or higher for the median IDR of the conventional construction (Point 1) is 24.0%. On the other hand, the probability of DS_1 or higher for the median IDR of the unibody design (Point 2, with a median IDR 6.1 times smaller) is significantly reduced to essentially 0%.

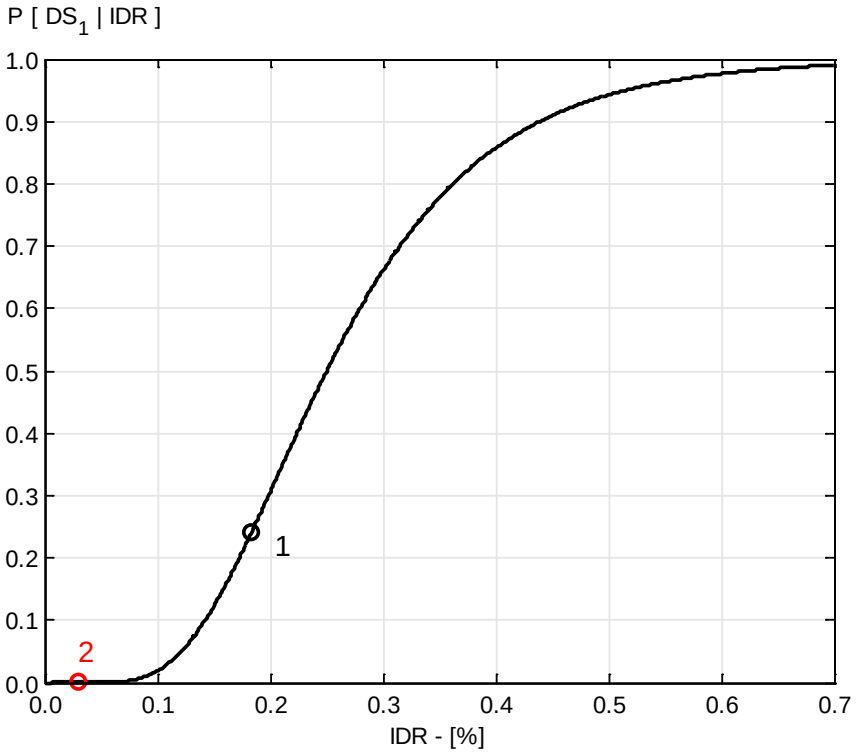

Fig. 3 – Fragility curve from ATC-58 project for DS_1 of light framed wood shear walls with structural panel sheathing, exterior stucco finish and interior gypsum wallboard, designed with hold-downs. Point 1 corresponds to the median IDR of conventional construction and Point 2 to the median IDR of the unibody approach, both for a magnitude 7.0 earthquake and distance 2 km, using the GMPE by Boore et al. [27].

2.3 Influence of Source-to-Site Distance on Probability of Damage

The previous sections have shown the significant differences between conventional and unibody designs for an individual house. The following sections evaluate the benefits on a regional scale, considering houses at different distances from the rupture zone. It is well known that, generally speaking, seismic energy attenuates with the source-to-site distance, *R*. This geometric attenuation is often proportional to R^{-c}, where the coefficient *c* depends

on the period, event magnitude and considered GMPE, but it is roughly between 0.5 and 1.25 for periods shorter than 0.5 seconds and magnitudes between 5.0 and 8.0. Therefore, record parameters affecting the inelastic displacement demands estimations (S_a, S_d, S_v and PGV) rapidly attenuate for sites farther away from the source. This is translated into an attenuation of IDR with the source-to-site distance. An example of the attenuation of IDR for a magnitude 7.0 earthquake is presented in Fig. 4, for both the conventional construction (Fig. 4a), and the unibody design (Fig. 4b). In both cases, the median and the 16th/84th percentiles are shown to make explicit the probabilistic nature of the inelastic displacement demands at a given distance.

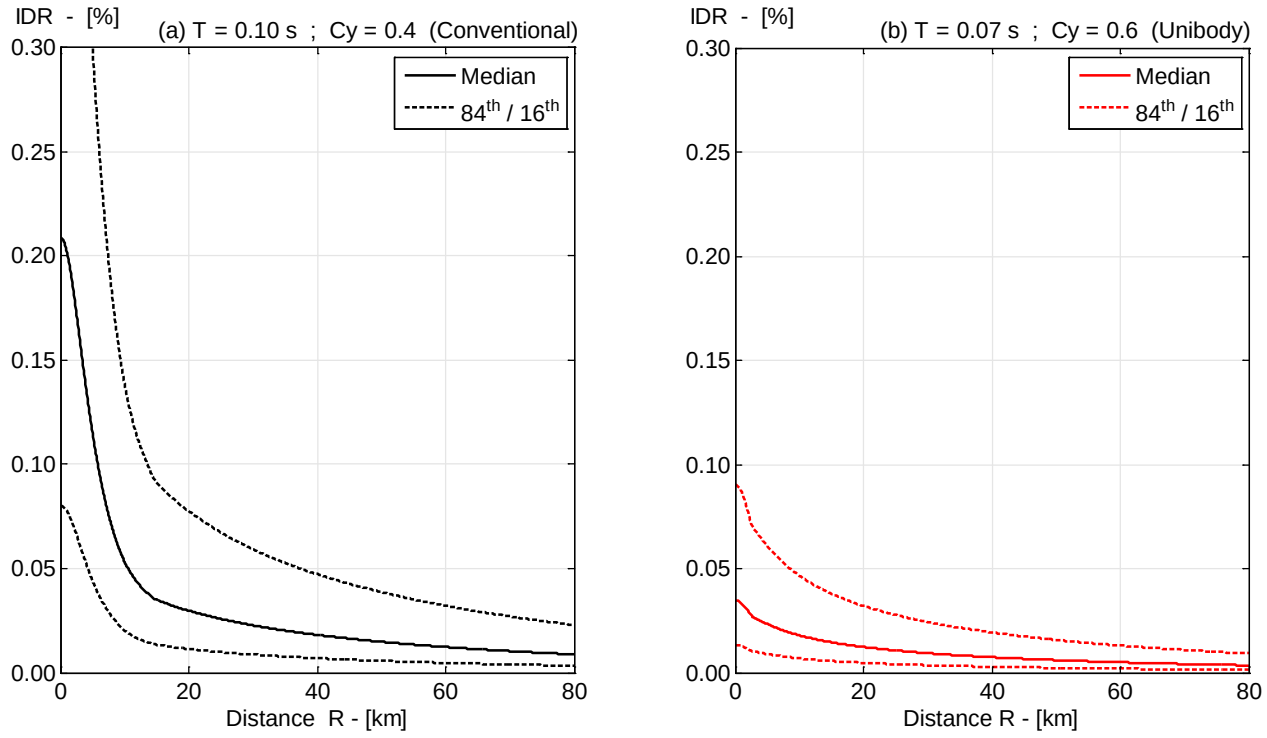

Fig. 4 – Attenuation of IDR for a magnitude 7.0 earthquake, using the GMPE by Boore et al. [27]. (a) Conventional construction. (b) Unibody construction.

The total probability of damage as a function of the source-to-site distance can be computed using the total probability theorem, as presented in Eq. (5).

$$P[DS_k \mid R=r] = \int_{idr} P[DS_k \mid idr] \cdot f_{IDR \mid R}(idr \mid R=r)\, d(idr) \tag{5}$$

At each distance r, the probability density function of IDR, $f_{IDR \mid R}(idr \mid R=r)$, is integrated with the probability of having a certain damage state k or higher given IDR, $P[DS_k \mid idr]$ (see Fig. 3) to obtain the total probability of damage state k or higher. The resulting probability for damage state 1 (DS_1) or higher is presented as a function of distance in Fig. 5. As can be noted, the probability when using unibody design is, as a general trend, 1 order of magnitude smaller than the one when using conventional construction. For example, at a source-to-site distance of 2 km, the probability of damage state 1 decreases from 38.4% to 2.1% (18.3 times), and at 15 km, it decreases from 3.1% to 0.3% (10.3 times). Moreover, the same probability of damage is presented at much closer distances when using the unibody approach. For example, unibody houses farther than 6.3 km from the source have a probability of damage smaller than 1%, while the same happens at 32.3 km in houses with conventional construction (distance reduced by 5.1 times).

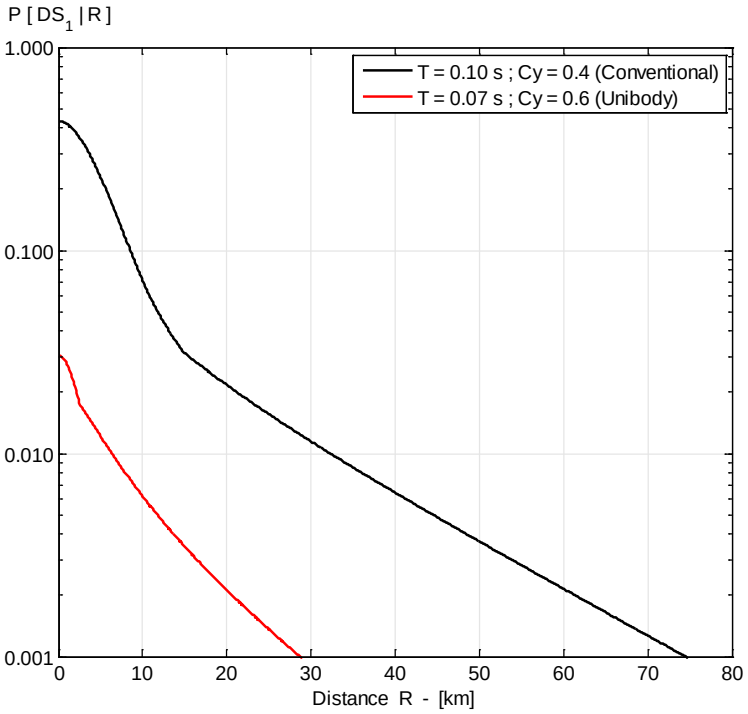

Fig. 5 – Probability of damage state 1 or higher (see Fig. 3 for fragility curve) as a function of source-to-site distance for the conventional and the unibody construction approaches, for a magnitude 7.0 earthquake and using the GMPE by Boore et al. [27]. The unibody design presents 1 order of magnitude smaller probability values.

2.4 Influence of Source-to-Site Distance on Affected Area and Number of Houses

Clearly, larger source-to-site distances are related to larger affected areas. For instance, if the earthquake source is modeled as a point source, the affected area can be easily computed from the distance with Eq. (6):

$$A = \pi \cdot R^2 \tag{6}$$

where A is the affected area and R is the source-to-site distance. In this case, the affected area is a function of the square of the distance. This means that a reduction of 5.1 times (like the reduction in the previous section for 1% probability of damage) in distance represents a reduction in the affected area of 26.0 times. Nevertheless, strike-slip earthquake rupture zones, for example, are commonly modeled as line sources, thus the affected area is not directly proportional to the square of the distance. In the example of the previous sections, the earthquake magnitude was 7.0, which corresponds to a strike-slip rupture zone of about 43 km long, using the Wells and Coppersmith [29] empirical relationships. Fig. 6 shows the affected area with a minimum probability of damage of 1%. As presented in the previous section, this threshold is achieved at 32.3 km from the source when using conventional construction and 6.3 km when using unibody construction. It can be observed in Fig. 6 that the affected area with the same minimum probability of damage is significantly reduced from 6,060 km^2 for the conventional construction, to 670 km^2 for the unibody approach. This represents a reduction of more than 9.0 times, when the reduction in distances was 5.1 times.

Note that Fig. 6 only compares the affected areas with the same minimum probability of damage. Not only is this area significantly reduced when using unibody design, but it should also be noted that the maximum probability of damage (at 0 distance) in the unibody area is significantly reduced (see Fig. 5). In this example, houses inside the conventional construction area of Fig. 6 have probabilities of damage ranging between 1% and 43%, while houses inside the unibody area have probabilities of damage between 1% and 3%. To account for

this difference, the expected value of the affected area with damage state 1 or higher can be computed as shown in Eq. (7).

$$E[A_1] = \int_r L(r) \cdot P[DS_1 \mid R = r]\, dr \tag{7}$$

where $L(r)$ is the total contour length at a distance r around the rupture zone and $P[DS_1 \mid R = r]$ is the probability of damage state 1 or higher at a given distance $R = r$, given in Fig. 5. For line sources, $L(r)$ can be obtained as a function of the rupture length, L_r, as presented in Eq. (8).

$$L(r) = 2\pi \cdot r + 2 \cdot L_r \tag{8}$$

The integral of Eq. (7) can be computed for both probability curves of Fig. 5 to compare the expected areas with damage state 1 or higher when using both construction approaches. The rupture length for this example (magnitude 7.0 earthquake) is 43 km, as mentioned before. Eq. (7) results in an expected affected area with damage state 1 or higher of 450 km^2 when using conventional construction, which is reduced to 30 km^2 (by 15.0 times, or a reduction of 93%) when using unibody design.

Assuming a certain constant density of houses throughout the area, the reduction in affected area corresponds to a reduction in the number of affected houses. This means that using a unibody approach can reduce the expected number of damaged houses by 15 times (or a reduction of 93%) for this scenario earthquake. In the same line, houses outside the marked areas in Fig. 6 have probabilities of damage lower than 1%, therefore virtually damage-free. Therefore, the area of damage-free houses for this scenario earthquake is increased by 5,390 km^2. Once again, this increment can be easily translated into an increment in the number of damage-free houses, increasing the resilience of the region. These types of information are useful for evaluating new public policies and resilience of seismic regions.

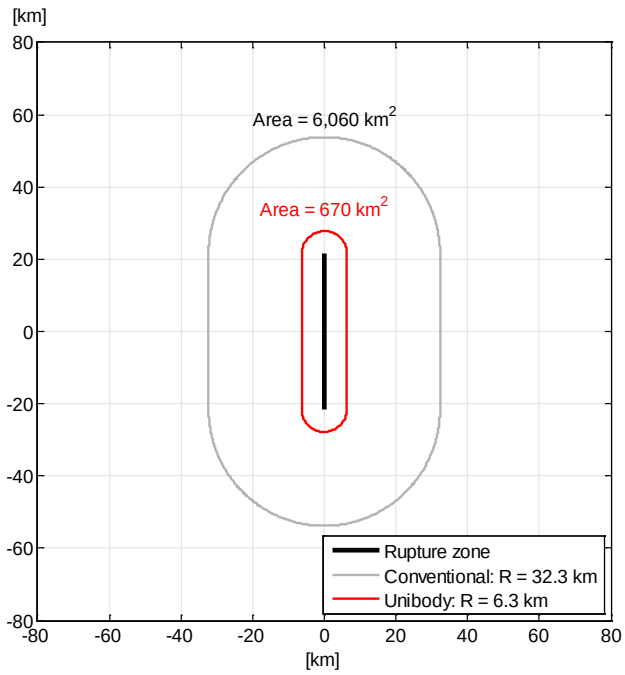

Fig. 6 – Affected areas by the same minimum probability of damage (1%) for a magnitude 7.0 earthquake and using the GMPE by Boore et al. [27]. (a) Conventional construction. (b) Unibody construction.

3. Discussion

The previous section has presented the benefits of using an enhanced design which increases the lateral strength, and more importantly, the lateral stiffness of houses, on a regional scale. Nonetheless, the unibody approach is not the only way for improving the residential resilience of urban areas located in seismic regions. However, the unibody approach is one that from a cost-benefit perspective can achieve large benefits with minimal costs for new residential construction [16 – 20]. Here, specific values of increments in strength and stiffness were used, however the proposed approach is general and can, of course, be used with other parameters [30].

4. Conclusions

This paper proposes a framework for assessing, at a regional scale, the use of an enhanced design for new residential construction. The framework is illustrated by evaluating the large benefits in improving the resilience of urban areas when using the "unibody design", which integrates and takes advantage of wall finishes to significantly increase the lateral stiffness and lateral strength of lowrise lightweight residential construction. The benefit in terms of reduction in the number of damage residential units is very large, which is the result of a series of multiplicative nonlinear effects:

1. Increasing the lateral strength and lateral stiffness of a structure, translates into reductions in lateral displacement demands. These reductions in general are not linearly proportional to the increase in strength or in stiffness. Moreover, these reductions are maximized in short-period structures. For example, unlike taller structures built on firm soils where doubling the lateral stiffness will typically translate in reductions in displacement demands between 20% and 40%, for short period structures the same increment in lateral stiffness will typically translate in a reduction of displacement demands of 40% to 60%. Furthermore, unlike medium- and long-period structures where increments in lateral strength on average do not lead to significant reductions in lateral deformations demands, for low-strength short-period structures an increment of lateral strength of 50% is translated into reductions of lateral deformation as large as 60%. The total reductions in lateral displacement demands resulting from combining the reductions achieved from the increments in strength and stiffness could be as large as 80%.
2. Decreasing the lateral inelastic displacement demands significantly reduces the probability of damage. This is because the relationship between lateral deformation demands and probability of experiencing a certain damage state is typically strongly nonlinear. For the structures analyzed in this study, a reduction of lateral displacement demands of 80% results in 18.3 times smaller probability of damage.
3. Ground motion intensity decreases rapidly and nonlinearly with distance. For example, spectral ordinates are roughly proportional to $R^{-1.0}$ where R is the distance to the horizontal projection of the rupture. This means that houses with conventional construction would experience a 1% or higher probability of being damaged if they are located on average within 30 km of the rupture of a M7 event, but now need to be on average at 6 km of the rupture to have the same probability. In other words, unibody houses would need to be 5 times closer to the rupture to experience the same probability of being damaged in the earthquake as conventional houses.
4. The area containing ground motions exceeding an intensity large enough to cause damage in houses, and therefore the potential number of damaged houses (assuming an approximately uniform density of houses in such area) is related to the square mean distance to the rupture required to trigger the damage. This means that shortening the distance at which houses will be potentially damaged from 30 to 6 km (5 times reduction) results in a reduction by 9 times in the area where the ground motion is large enough to cause damage. Moreover, the expected area of damaged houses is reduced by 15 times (reduction of 93%).

It is then clear that the novel "unibody design" takes full advantage of these series of nonlinear effects that are translated into very large potential benefits in the reduction of the number of displaced families from their residences, and in the economic losses associated with repairs, therefore significantly increasing the resilience of urban areas located in seismic regions.

5. Acknowledgements

This study was inspired and has greatly benefited from a previous research investigation of the second author with Professors Greg Deierlein and Benjamin Fell and graduate students Scott Swensen, Cristian Acevedo, Ezra Jampole and Amy Hopkins in which, with financial support from the U.S. National Science Foundation, the "unibody design" concept was developed and experimentally tested. Their collaboration and comments are greatly appreciated. Authors would also like to acknowledge *CONICYT – Becas Chile*, the *Nancy Grant Chamberlain Fellowship*, the *Charles H. Leavell Fellowship* and the *Shah Graduate Student Fellowship* for the financial support of the doctoral studies of the first author at Stanford University under the supervision of the second author. The authors would also like to acknowledge the partial financial support by the John A. Blume Earthquake Engineering Center at Stanford University to attend this conference.

6. References

[1] Earthquake Engineering Research Institute (EERI), International Association for Earthquake Engineering (IAEE). World Housing Encyclopedia (WHE). *Retrieved April 20, 2016, from* http://www.world-housing.net/

[2] New Zealand Ministry for Culture and Heritage, Manatu Taonga (2013): Housing – Te Ara Encyclopedia of New Zealand. *Retrieved April 20, 2016, from* http://www.teara.govt.nz/en/housing/

[3] Comerio MC (1995): Northridge housing losses. *A study for the California Governor's Office of Emergency Services. Research Report, Center for Environmental Design Research, University of California,* Berkeley, CA, USA.

[4] Comerio MC (1997): Housing issues after disasters. *Journal of Contingencies and Crisis Management*, ***5*** (3), 166–178.

[5] Comerio MC, Landis JD, Firpo CJ, Monzon JP (1996): Residential earthquake recovery. *California Policy Seminar, University of California*, Berkeley, CA, USA.

[6] Hall JF, Schmid B, Comerio MC, Russell J, Quadri ND, Harder R, Powell B, Hamburger R, Steinberg R (1996): Wood buildings. *Earthquake Spectra*, ***12*** (S1), 125–176.

[7] Kircher CA, Reitherman RK, Whitman RV, Arnold C (1997): Estimation of earthquake losses to buildings. *Earthquake Spectra*, ***13*** (4), 703–720.

[8] McClure FE (1973): Performance of single family dwellings in the San Fernando Earthquake of February 9, 1971. *Report prepared for the National Oceanic and Atmospheric Administration and supported by the Department of Housing and Urban Development.*

[9] Steinbrugge KV, Schader EE, Bigglestone HC, Weers CA (1971): San Fernando Earthquake, February 9, 1971. *Pacific Fire Rating Bureau, San Francisco, CA, USA.*

[10] Jennings PC (1997): Enduring lessons and opportunities lost from the San Fernando earthquake of February 9, 1971. *Earthquake Spectra*, ***13*** (1), 25–44.

[11] Kircher CA, Seligson HA, Bouabid J, Morrow GC (2006): When the Big One strikes again—Estimated losses due to a repeat of the 1906 San Francisco earthquake. *Earthquake Spectra*, ***22*** (S2), 297–339.

[12] Porter KA, Scawthorn CR, Beck JL (2006): Cost-effectiveness of stronger woodframe buildings. *Earthquake Spectra*, ***22*** (1), 239–266.

[13] Filiatrault A, Christovasilis IP, Wanitkorkul A, Van De Lindt JW (2010): Experimental seismic response of a full-scale light-frame wood building. *Journal of Structural Engineering*, ***136*** (3), 246–254.

[14] Filiatrault A, Fischer D, Folz B, Uang CM (2002): Seismic testing of two-story woodframe house: Influence of wall finish materials. *Journal of Structural Engineering*, ***128*** (10), 1337–1345.

[15] Uang CM, Gatto K. (2003): Effects of finish materials and dynamic loading on the cyclic response of woodframe shearwalls. *Journal of Structural Engineering*, ***129*** (10), 1394–1402.

[16] Swensen S, Acevedo C, Jampole E, Miranda E, Deierlein G, Hopkins A, Fell B (2014): Toward damage free residential houses through unibody light-frame construction with seismic isolation. *SEAOC 83rd Annual Convention*. Indian Wells, CA, USA.

[17] Swensen S, Deierlein G, Miranda E (2015): Behavior of screw and adhesive connections to gypsum wallboard in wood and cold-formed steel-framed wallettes. *Journal of Structural Engineering*, *E4015002*.

[18] Swensen S, Deierlein G, Miranda E, Fell B, Acevedo C, Jampole E (2014): Finite element analysis of light-frame unibody residential structures. *10th U.S. National Conference on Earthquake Engineering*. Anchorage, AK, USA.

[19] Acevedo C, Deierlein G, Miranda E, Fell B, Swensen S, Jampole E (2016): Experimental testing of full-scale unibody wood-frame room. Submitted for evaluation and possible publication to *Journal of Structural Engineering*.

[20] Acevedo C, Deierlein G, Miranda E, Fell B, Swensen S, Jampole E (2016): Shake table testing of a full-scale two-story unibody wood-frame house. Submitted for evaluation and possible publication to *Journal of Structural Engineering*.

[21] May PJ (2007): Societal implications of performance-based earthquake engineering. *PEER Report 2006/12*, Pacific Earthquake Engineering Research Center, Berkeley, CA, USA.

[22] Camelo V (2003): Dynamic characteristics of woodframe buildings. *Ph.D. Thesis. California Institute of Technology*, Pasadena, CA, USA.

[23] Graizer V, Kalkan E (2009): Prediction of spectral acceleration response ordinates based on PGA attenuation. *Earthquake Spectra*, ***25*** (1), 39–69.

[24] Ruiz-García J, Miranda E (2003): Inelastic displacement ratios for evaluation of existing structures. *Earthquake Engineering & Structural Dynamics*, ***32*** (8), 1237–1258.

[25] Ruiz-García J, Miranda E (2007): Probabilistic estimation of maximum inelastic displacement demands for performance-based design. *Earthquake Engineering & Structural Dynamics*, ***36*** (9), 1235–1254.

[26] Akkar S, Miranda E (2004): Improved displacement modification factor to estimate maximum deformations of short period structures. *13th World Conference on Earthquake Engineering* (Paper No. 3424), Vancouver, Canada.

[27] Boore DM, Stewart JP, Seyhan E, Atkinson GM (2014): NGA-West2 equations for predicting PGA, PGV, and 5% damped PSA for shallow crustal earthquakes. *Earthquake Spectra*, ***30*** (3), 1057–1085.

[28] Hamburger R, Rojahn C, Moehle J, Bachman R, Comartin C, Whittaker A (2004): The ATC-58 project: Development of next-generation performance-based earthquake engineering design criteria for buildings. *13th World Conference on Earthquake Engineering* (Paper No. 1819), Vancouver, Canada.

[29] Wells DL, Coppersmith KJ (1994): New empirical relationships among magnitude, rupture length, rupture width, rupture area, and surface displacement. *Bulletin of the Seismological Society of America*, ***84*** (4), 974–1002.

[30] Heresi P, Miranda E (2016): Quantitative evaluation of benefits at the regional level of new strategies to improve the seismic performance of low-rise residential construction. Submitted for evaluation and possible publication to *Earthquake Spectra*. Earthquake Engineering Research Institute.